

Chiral incommensurate phase from three spin interactions in an optical lattice

Christian D'Cruz¹ and Jiannis K. Pachos²

¹*Department of Mathematics, Royal Holloway,
University of London, Egham, Surrey TW20 0EX, UK**

²*Department of Applied Mathematics and Theoretical Physics,
University of Cambridge, Cambridge CB3 0WA, UK†*

(Dated: May 24, 2019)

A spin-1/2 chain model that includes three spin interactions can effectively describe the dynamics of an optical lattice with a semi-one dimensional configuration. A perturbative theoretical approach and numerical study of its ground state is performed that reveals a rich variety of phases and criticalities. We establish a range of parameters, corresponding to a large degeneracy present between phases with period 2 and 3, that nests a gapless incommensurate chiral phase.

PACS numbers: 05.30.Jp,75.30.Fv

I. INTRODUCTION

The proposal [1] and subsequent realization [2–4] of optical lattices for the manipulation of ultra-cold atoms has attracted a great deal of research towards the implementation of quantum computation [5–7] and the simulation of condensed matter systems [8–12]. The main advantages of optical lattices are their long decoherence times and high degrees of controllability. Hence, one is able to probe phenomena that manifest themselves at higher orders in perturbation theory such as many body interactions [13]. This gives the possibility to engineer and control exotic interactions in many body systems and subsequently realize novel phases of matter. Examples include cases where frustration effects are present or competing phenomena coexist giving rise to large degeneracy structures [14, 15]. Towards this direction we consider a semi-one dimensional lattice comprising a triangular ladder. The dynamics of two boson species mounting the optical lattice in the limit of strong collisional interactions can be effectively described by a chain of spin-1/2 interacting particles. Here we consider systems with two and three spin interactions given by $ZZ = \sum_i \sigma_i^z \sigma_{i+1}^z$ and $ZZZ = \sum_i \sigma_i^z \sigma_{i+1}^z \sigma_{i+2}^z$ respectively. We shall see explicitly that it is possible to make ZZZ dominant by appropriate tuning of the collisional and tunnelling couplings. As simple as these interactions may seem, when combined, they give rise to a rich

variety of phase transitions, the study of which is the subject of this article.

In particular, we consider a Hamiltonian that includes the two and three spin interactions with couplings λ_1 and λ_2 respectively, in the presence of a transverse field with unit amplitude. We observe that for $\lambda_2 = 0$ the model is exactly solvable, as it reduces to the Ising interaction with critical points at $\lambda_1 = \pm 1$. For $\lambda_1 = 0$ we obtain a Hamiltonian that is not analytically diagonalizable. Nevertheless, a numerical study reveals a tricritical point at $\lambda_2 = 1$ that is in the same universality class as the three-state Potts model [16]. When the two spin interaction is dominant the ground state has a spin-order of period 2 while the dominance of the higher order interaction brings about a spin-order of period 3. Though these phases are gapped, there are values of relative couplings where these orders compete, giving rise to a high degree of degeneracy. This characteristic allows for the presence of a gapless incommensurate chiral phase that extends to a wide range of parameters. In Figure 1 the fidelity of the actual ground state of the Hamiltonian is plotted against the ground state of each individual term comprising it. While we see that these agree for a large range of couplings there is an area between spin-order 2 and 3 where these states fail to accurately describe the nature of the system. We shall identify this as the gapless incommensurate chiral phase. A similar region has been presented by Fendley, Sengupta and Sachdev [14] in a 1-dimensional hard boson system.

The article is organized as follows. In Section II we present the realization of the two and three spin interactions by ultra-cold atoms superposed by optical lattices. Section III is a study of the tricritical point

*Electronic address: C.H.D-Cruz@rhul.ac.uk

†Electronic address: j.pachos@damtp.cam.ac.uk

present at $\lambda_1 = 0$, $\lambda_2 = 1$. In Section IV, we present the properties of the full Hamiltonian. For that we employ perturbation theory, a bosonization of the model and a study of an effective field theory that eventually reveal the incommensurate chiral phase. Finally, in Section V, we conclude and present future directions.

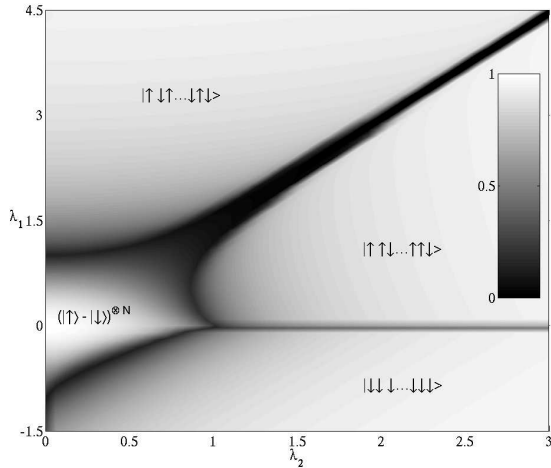


FIG. 1: A plot of the fidelity of the ground state $|\psi\rangle$ with the predictions obtained from each individual term of the Hamiltonian. The state $|\uparrow\uparrow\downarrow\downarrow\rangle$ corresponds to ZZ, $|\uparrow\uparrow\downarrow\downarrow\rangle$ corresponds to ZZZ and $(|\uparrow\rangle - |\downarrow\rangle)^{\otimes N}$ corresponds to the transverse field. The state $|\downarrow\downarrow\downarrow\downarrow\rangle$ is the common ground state of ZZ and ZZZ for this range of couplings.

II. OPTICAL LATTICES AND THREE SPIN INTERACTIONS

Consider the physical setup where an ultra-cold atomic cloud of two different species, a and b , is

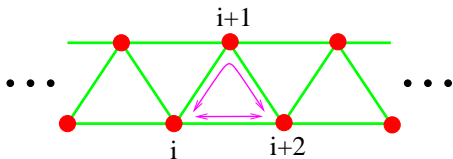


FIG. 2: The one dimensional chain constructed out of equilateral triangles. Three-spin interaction terms appear, e.g. between sites i , $i+1$ and $i+2$ as for example tunnelling between i and $i+2$ can happen through two different paths, directly and through site $i+1$, the latter resulting into an exchange interaction between i and $i+2$ that is influenced by the state of the site $i+1$.

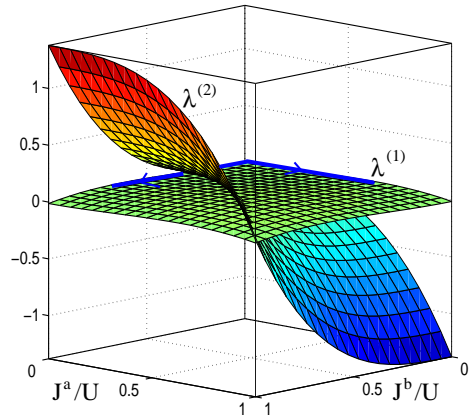


FIG. 3: The effective couplings λ_1 and λ_2 are plotted against J^a/U and J^b/U for $U_{aa} = U_{bb} = 2.12U$ and $U_{ab} = U$. The coupling λ_1 appears almost constant and zero as the unequal collisional couplings can create a plateau area for a wide range of the tunnelling couplings, while λ_2 can be varied freely to positive or negative values.

superposed with a three dimensional optical lattice. The atoms can tunnel through the potential barriers of the lattice from one site to the next with a coupling J . When two or more atoms are present in the same site, they collide with coupling U . For sufficiently large intensities of the laser radiation, where $J \ll U$, the system is in the Mott insulator regime with a regular number of atoms per site. In particular, we can arrange the density of the atomic cloud to be low enough so that only one atom can exist at each site of the lattice, i.e. $\langle n_a + n_b \rangle \approx 1$. In this way each lattice site is a simple two state system, that can be viewed as a spin-1/2 particle. Within this representation, the Hamiltonian can be written in terms of Pauli spin operators.

Indeed, for the triangular ladder seen in Figure 2 we obtain the Hamiltonian of the form [13, 17]

$$H = B \sum \sigma_i^x + \lambda_1 \sum \sigma_i^z \sigma_{i+1}^z + \lambda_2 \sum \sigma_i^z \sigma_{i+1}^z \sigma_{i+2}^z, \quad (2.1)$$

where B , λ_1 and λ_2 are all functions of the initial tunnelling and collisional couplings, J and U . The values of λ_1 and λ_2 can be controlled independently by varying J and U . In particular, it is possible to make λ_2 large compared to λ_1 as can be seen in Figure 3. A careful consideration of the system would reveal that terms of the form $\sigma_i^z \sigma_{i+2}^z$ also appear, due to the triangular configuration. This can be remedied by employing superlattices that do not alter the

other terms.

III. THE ZZZ INTERACTION

Ultimately, we would like to study the entire (λ_1, λ_2) plane, identify the regions of criticality behavior and understand the global properties of the ground state. Before turning to the general problem let us consider the two special limiting cases. Initially, when $\lambda_2 = 0$, the Hamiltonian reduces to the Ising interaction between neighboring spins in the presence of a transverse magnetic field. This well-studied model exhibits criticality behavior for $\lambda_1 = \pm 1$.

Another interesting model [18] can be obtained for $\lambda_1 = 0$. For simplicity we can take $\lambda_2 = 1$ and consider the Hamiltonian to be a function of the transverse field with amplitude B [19, 20]. As we vary B we observe that there are two distinctive regions. For $B \gg 1$, the ground state has all the spins oriented towards the x direction, and for $B \ll 1$ there is a degeneracy between the states $|\uparrow\uparrow\uparrow\uparrow\uparrow\uparrow\uparrow\rangle$, its translations (the Z_3 symmetry) and $|\downarrow\downarrow\downarrow\downarrow\downarrow\downarrow\downarrow\rangle$. It is of interest to study the behavior of the system between these two limiting cases.

Due to the symmetry of the Hamiltonian we can pinpoint where a possible critical point can lie. For that, one can define, $\mu_i^x \equiv \sigma_i^z \sigma_{i+1}^z \sigma_{i+2}^z$ and $\mu_i^z \equiv \prod_{n=0}^{\infty} \sigma_{i-3n}^x \sigma_{i-3n-1}^x$. It is easily verified [21] that these operators obey the Pauli algebra commutation relations. Moreover, under this transformation the Hamiltonian becomes $BH(B^{-1})$ which has exactly the same spectrum as $H(B)$. Hence, if there exists a single critical point it has to be at $B = 1$.

We can verify this numerically and identify the critical exponents, by observing the minimum in the energy gap between the ground and first excited state on a finite chain of spins with periodic boundary conditions. In the thermodynamical limit this minimum, if it corresponds to a critical point, will become zero. Near this region the energy gap, Δ , is expected to scale as follows [22],

$$\Delta = N^{-z} \Phi \left(N^{1/\nu} (B - B_c) \right). \quad (3.1)$$

Here Φ is a universal scaling function, z is the dynamic critical exponent, and ν is the correlation length exponent. Figure 4(a) gives a plot of $N^{1.00263} \Delta$ versus B , which shows that the energy minimum progresses towards $B = 1$ for increasing N . We may employ Eqn. (3.1) to estimate z and ν . Figure 4(b) shows $N^{1.0002623} \Delta$ against

$N^{1/0.757868} (B_x - B_x^c)$, where the data for systems of different sizes come together into a single curve. From Eqn. (3.1) we deduce the value of the critical exponents to be $z \approx 1$ and $\nu \approx 0.76$.

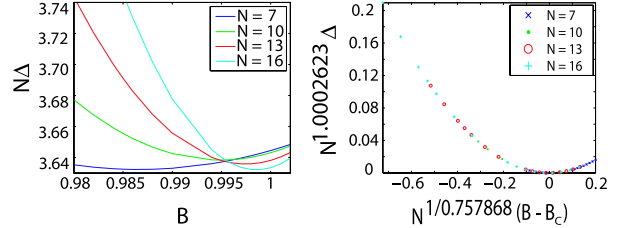


FIG. 4: (a) Quantum critical point signified by the minima of the energy gap Δ . Due to low N , these provide only an estimate for the position of the critical point. The progression towards $B_x = 1$ as N increases supports the theoretical predictions. (b) To determine the critical exponents we have chosen the values of z and ν that best superpose the curves of Figure 4(a) into one uniform function Φ .

We can also determine numerically the central charge of the critical theory and see if it corresponds to the same universality class. The central charge can be obtained by studying the scaling behavior of the entropy of entanglement [23]. The latter is given by the von Neumann entropy, S_L , of the reduced density matrix, ρ_L . It can be calculated from the density matrix of the original system, being in a pure state, where all but L contiguous spins are traced out. This indicates quantitatively the degree of entanglement of the L spins with the rest of the chain. Indeed, we have

$$\begin{aligned} \rho_L &\equiv \text{tr}_{N-L} |\psi\rangle\langle\psi|, \\ S_L &\equiv \text{tr}(\rho_L \log \rho_L), \end{aligned} \quad (3.2)$$

where $|\psi\rangle$ is the ground state of the system. For a critical configuration and for large L we expect $S_L \approx \frac{c+\bar{c}}{6} \log L$, where c is the central charge of the corresponding conformal field theory and \bar{c} is its complex conjugate. The central charge uniquely corresponds to the critical exponents of the energy and of the correlation length, z and ν , respectively. We know that for non-critical chains S_L should be saturated for large enough values of L . This behavior is observed from the simulations when $\lambda_2 \neq 1$. On the other hand, when we are at $\lambda_2 = B = 1$ we obtain Figure 5 that shows the expected logarithmic progression. By a logarithmic fitting we can deduce that $c \approx 4/5$. Hence, our model is in the same universality class as the three-state Potts model and

it corresponds to the critical exponents $z = 1$ and $\nu = 3/4$ in agreement with the earlier findings.

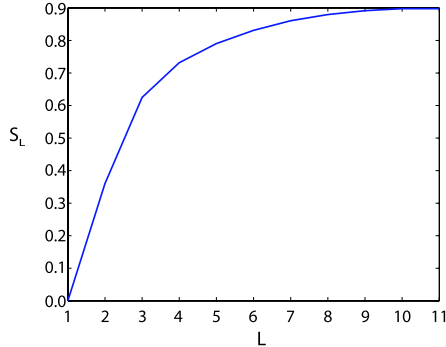


FIG. 5: Entropy of entanglement, S_L , as a function of L for a total of 19 spins. The plot shows a logarithmic behavior that indicates criticality for $\lambda_2 = 1$.

IV. THE FULL HAMILTONIAN

We can now turn to the full Hamiltonian for arbitrary values of the coupling parameters. For convenience we set $B = 1$ and vary only the interaction couplings λ_1 and λ_2 . Without loss of generality we can restrict on the $\lambda_2 > 0$ half-plane as the case $\lambda_2 < 0$ is automatically obtained by exchanging $\uparrow \leftrightarrow \downarrow$.

For large values of λ_1 or λ_2 it is possible to neglect the transverse field X and treat the system classically. We find two asymptotes along which the ground state should undergo a first order phase transition. By introducing X as a small perturbation one can predict how these curves behave when we approach the origin $\lambda_1 = \lambda_2 = 0$. We find that along the asymptote $\lambda_1/\lambda_2 = 3/2$ the classical ground state is highly degenerate: it is in fact infinitely degenerate in the thermodynamic limit. In the quantum regime, this gives rise to an intermediate region between the two phases with spin-order 2 and 3, the size and nature of which will be studied in this section.

A. Perturbation Theory

To understand the behavior of Hamiltonian (2.1) we shall employ perturbation theory. Surprisingly, the second order perturbation will give a very good approximation to the numerical findings shown in Figure 1.

1. Classical Regime

As a first step we take $\lambda_1, \lambda_2 \gg 1$, thus neglecting the X term the Hamiltonian reduces to

$$H \approx \lambda_1 \sum_i \sigma_i^z \sigma_{i+1}^z + \lambda_2 \sum_i \sigma_i^z \sigma_{i+1}^z \sigma_{i+2}^z. \quad (4.1)$$

This Hamiltonian has a classical behavior, so it can be solved exactly by examining eigenstates of $\sigma_z^{\otimes N}$. There are three regions on the (λ_1, λ_2) plane of distinct ground state behavior. Consider first $\lambda_1 < 0$, $\lambda_2 > 0$. The energy of the system is minimized uniquely by the state

$$|A\rangle = |\downarrow\downarrow\downarrow\downarrow\downarrow\downarrow \dots \downarrow\rangle. \quad (4.2)$$

From the expectation values, $\langle A | \sum_i \sigma_i^z \sigma_{i+1}^z | A \rangle / N = 1$ and $\langle A | \sum_i \sigma_i^z \sigma_{i+1}^z \sigma_{i+2}^z | A \rangle / N = -1$, one can calculate the energy per site to be $E_A = \lambda_1 - \lambda_2$. Similarly we take the cases of $\lambda_1 > 0$, $\lambda_2 \gg \lambda_1$ and $\lambda_1 > 0$, $\lambda_2 \ll \lambda_1$, resulting in the following ground states

$$|B\rangle = |\uparrow\uparrow\downarrow\uparrow\uparrow\downarrow \dots \downarrow\rangle, \quad (4.3)$$

with $E_B = -\frac{1}{3}\lambda_1 - \lambda_2$ and

$$|C\rangle = |\uparrow\downarrow\uparrow\downarrow\uparrow\downarrow \dots \downarrow\rangle, \quad (4.4)$$

with $E_C = -\lambda_1$. Observe that these states are 3 and 2 periodic respectively giving rise to Z_3 and Z_2 symmetries. To evaluate the position of the phase transitions we simply equate energies in neighboring regions. In this way we obtain the asymptotes $\lambda_1 = 0$ and $\lambda_1 = \frac{3}{2}\lambda_2$ that separate the states of the system $|A\rangle$, $|B\rangle$ and $|C\rangle$ as seen in Figure 6.

Another classical region is obtained at $\lambda_1, \lambda_2 \ll 1$, where the transverse field, X , dominates. In this region the ground state is given by

$$|D\rangle = |-\rangle^{\otimes N}, \quad (4.5)$$

with $|-\rangle \equiv (|\uparrow\rangle - |\downarrow\rangle)/\sqrt{2}$ and an energy per site of $E_D = -1$.

2. Quantum Regime

We now consider the transverse field as a perturbation to the theory, so we rewrite our Hamiltonian as

$$H = \lambda_2 \sum_i (\lambda \sigma_i^x + \mu \sigma_i^z \sigma_{i+1}^z + \sigma_i^z \sigma_{i+1}^z \sigma_{i+2}^z), \quad (4.6)$$

where $\lambda \equiv 1/\lambda_2$ and $\mu \equiv \lambda_1/\lambda_2$. Cyclic permutations of states $|B\rangle$ and $|C\rangle$ are also ground states of

the classical theory due to the translational invariance of the Hamiltonian. Nevertheless, we need not employ degenerate perturbation theory at this point since the permutations behave identically under the transverse field, X . For this Hamiltonian the energies per site are

$$\tilde{E}_A = \lambda_1 - \lambda_2 - \frac{1}{\lambda_2} \frac{1}{6 - 4\mu}, \quad (4.7)$$

$$\tilde{E}_B = - \left(\lambda_1 + \frac{\lambda_2}{3} \right) - \lambda_2 \left[\left(\frac{1}{9} \right) + \left(\frac{1}{3} \right) \frac{1}{6 + 4\mu} \right]. \quad (4.8)$$

By inspection we see that the two energies are equal for $\mu = 0$, which coincides exactly with the classical solution. Hence, at $\mathcal{O}(\lambda^2)$, the boundary between $|A\rangle$ and $|B\rangle$ remains unchanged, as seen in Figure 6.

Let us turn to the perturbation treatment of the boundary between the $|D\rangle$ and the $|A\rangle$ states. In fact, to the second order in the couplings, λ_1 and λ_2 , we find

$$\tilde{E}_D = -1 - \frac{\lambda_1^2}{4} - \frac{\lambda_2^2}{6}. \quad (4.9)$$

Equating $\tilde{E}_D = \tilde{E}_A$ we obtain the corresponding boundary to be a correction of the classical one given by $\lambda_1 = \lambda_2 - 1$. The computational solution of $\tilde{E}_D = \tilde{E}_A$ is given in Figure 6. It provides a line of second order phase transition joining the Potts critical point and the Ising critical point that fits firmly with the fidelity plot in Figure 1.

3. Competing Ground States

We saw above that for $\mu = \frac{3}{2}$ the period 2 and period 3 phases have the same ground state energy. Interestingly, on this asymptote the two spin-orders can mix, giving rise in the thermodynamic limit to an infinitely degenerate ground state. A perturbation theory around this area is non-trivial as care has to be taken in the way the degeneracy is lifted. Using a bosonization procedure similar to that presented in [14], we will calculate the spectrum of the theory up to second order in the transverse field. We will find a finite intermediate phase separating the period 2 and period 3 gapped phases.

Let us present in detail the bosonization procedure necessary to develop the perturbation theory. Consider two new types of bosons – the 3, created by the t^\dagger operator, and 2, created by p^\dagger . In the spin formalism, 3 corresponds to $\uparrow\uparrow\downarrow$, while 2 is equivalent to $\uparrow\downarrow$.

Thus,

$$|B\rangle = |33\dots 3\rangle \text{ and } |C\rangle = |22\dots 2\rangle. \quad (4.10)$$

All states that are composed of 2s and 3s are degenerate along the line $\mu = \frac{3}{2}$. Therefore, the region of the phase diagram that we want to study is given by

$$0 < |\mu - 3/2| \ll |\lambda_1|, |\lambda_2|. \quad (4.11)$$

Since there are no first order contributions in the perturbation theory, the region we want to study can be parameterized by

$$\mu = \frac{3}{2} + \sigma\lambda^2, \quad (4.12)$$

for a dimensionless parameter σ .

The approach is to create a theory with t and p bosons that is equivalent to the present one. Let us first work with t bosons. The vacuum state has the form $|22\dots 2\rangle$, with no 3s. To construct the Hamiltonian we need the self energy of a t boson, the interaction energy and the hopping amplitude. For that, we calculate the energies per site needed to add 22, 33 and 23 bonds, given by E_{22} , E_{33} and E_{23} , respectively. For example,

$$\underbrace{|23\dots 23\rangle}_{2(N-1)} \rightarrow \underbrace{|23\dots 2323\rangle}_{(2N)} \quad (4.13)$$

gives rise to the energy gap $2E_{23}$.

Up to order $\mathcal{O}(\lambda^2)$, these quantities are given by

$$\begin{aligned} E_{22} &= -2\mu + \frac{\lambda^2}{2(1-2\mu)}, \\ E_{33} &= -(3+\mu) - \frac{\lambda^2}{3}, \\ E_{23} &= -\frac{3}{2}(1+\mu) - \frac{\lambda^2}{6}. \end{aligned} \quad (4.14)$$

Consider now the energy, E_t , of a t boson in a background of 2s. This can be evaluated by considering the change

$$|22222\rangle \rightarrow |2323\rangle, \quad (4.15)$$

where we have kept the same length in the two spin chains. Hence, we can evaluate

$$\begin{aligned} E_t &= 2E_{23} - \frac{5}{2}E_{22} = \lambda^2 \left(\frac{7}{24} + 2\sigma \right), \\ E_{t,int} &= -\frac{\lambda^2}{4}. \end{aligned} \quad (4.16)$$

Finally, we calculate the hopping amplitude, which is given by the activation energy needed to perform the exchange

$$|23\rangle \rightarrow |32\rangle.$$

This has a value of $-\frac{\lambda^2}{6}$. We are now in a position to rewrite the Hamiltonian, which takes the following form

$$\begin{aligned} H = & \frac{N}{2} \left(-2\mu + \frac{\lambda^2}{2(1-2\mu)} \right) \\ & - \lambda^2 \sum_l \left[\frac{1}{6} (t_{l+2}^\dagger t_l + t_l^\dagger t_{l+2}) \right. \\ & \left. - t_l^\dagger t_l \left(\frac{7}{24} + 2\sigma \right) + \frac{1}{4} t_{l+3}^\dagger t_l^\dagger t_{l+3} t_l \right]. \end{aligned} \quad (4.17)$$

The label l is over the original indices, with a t boson being centered in the middle of the 3 deformation. We consider $\sigma \gg 1$, which corresponds to the spin-order 2 phase. The ground state is the vacuum state $|22\dots 2\rangle$, which is in agreement with original analysis. The lowest excited energy is $\lambda^2 (2\sigma - \frac{1}{24})$ above the vacuum state. Thus at $\sigma = \frac{1}{48}$ a phase transition occurs from period 2 to the intermediate region.

Following the same procedure we can find the boundary of the period 3 gapped phase. Now the vacuum state is $|33\dots 3\rangle$ and the relevant energies are with respect to the p boson. We have

$$\begin{aligned} E_p &= 2E_{23} - \frac{5}{3}E_{33} = \lambda^2 \left(-\frac{4}{3}\sigma + \frac{2}{9} \right), \\ E_{p,int} &= -\frac{\lambda^2}{4}, \end{aligned} \quad (4.18)$$

while the hopping amplitude is the same. In terms of these variables the Hamiltonian takes the form

$$\begin{aligned} H = & -\frac{N}{3} \left(3 + \mu + \frac{\lambda^2}{3} \right) \\ & - \lambda^2 \sum_l \left[\frac{1}{6} (p_{l+3}^\dagger p_l + p_l^\dagger p_{l+3}) \right. \\ & \left. + p_l^\dagger p_l \left(\frac{4}{3}\sigma - \frac{2}{9} \right) + \frac{1}{4} p_{l+2}^\dagger p_l^\dagger p_{l+2} p_l \right]. \end{aligned} \quad (4.19)$$

An identical analysis is now necessary, by simply considering $\sigma \ll -1$. The p bosons cost large positive energy, making the ground state the vacuum, as one would expect. The first excited state has an energy of $-\lambda^2 (\frac{4}{3}\sigma + \frac{7}{9})$, so the boundary is at $\sigma = -\frac{7}{12}$.

We therefore have a prediction of the width of the intermediate phase that is illustrated in Figure 6.

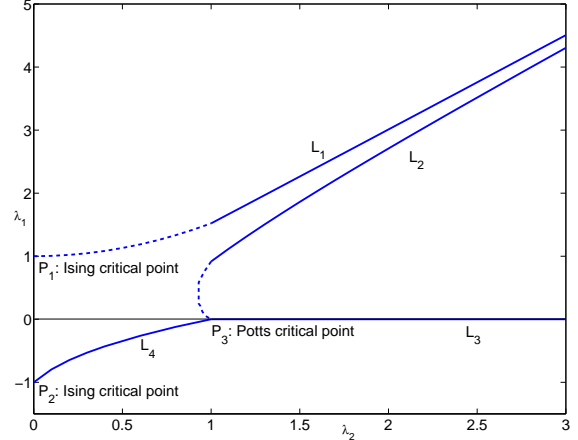


FIG. 6: An outline of the perturbative results is given by the solid lines. Dotted lines are inserted by hand for completion. There are three disjoint regions of different periodicity, separated by lines of phase transitions, of both first (L_3) and second order (L_1 , L_2 and L_4).

This result is in perfect agreement with the fidelity plot in Figure 1.

B. Criticality Behavior

At this point we can discuss the criticality behavior of our system. Apart from the Ising critical points, P_1 and P_2 , and the three-state Potts model critical point, P_3 , we can identify the critical behavior of the lines, L_1 , L_2 , L_3 and L_4 , seen in Figure 6, where our results of the perturbation treatment are summarized.

Specifically, we obtain first order critical behavior for $\lambda_1 = 0$ and $\lambda_2 > 1$ and second order behaviors for the rest of the curves. The perturbation theory shows that the line, L_3 , acquires no second order contribution indicating its first order nature. This is also supported by a numerical study of the energy gap for a chain of 19 spins. Indeed, we find that its minima lie along lines similar to the ones in Figure 6. Furthermore, there is an actual energy crossing along the first order line while all the other critical points remain gapped.

Studying the critical exponents along the line L_4 we find that in moving from P_3 to P_2 along the line of criticality, the exponent z decreases to zero and becomes discontinuous at the point P_2 . Moving in the other direction along L_2 yields ever increasing values of z . Hence, in view of Eqn. (3.1), we confirm that as the transverse field becomes insignificant, the

phase transitions return to first order behavior with an actual energy level crossing. Along the upper asymptote, L_1 , we observe similar behavior. The critical exponent is large in configurations far away from the origin and decreases continuously down to $z = 1/2$ at the Ising critical point P_1 .

These results present a rich variety of phase transition behavior. From Figures 1 and 6 we see that the second order perturbation theory gives a good picture of the ground state of the full Hamiltonian in most of the parametric region. The only part of the (λ_1, λ_2) plane that is not yet understood is the strip bounded by the lines, L_1 and L_2 . Probing the physics of this region is the subject of the next subsection.

C. Incommensurate Phase

It becomes apparent from the previous that perturbation theory cannot give reliable information about the physics between, L_1 and L_2 . To study that region we resort to the Landau-Ginzburg approximation [24]. As we shall see, the resulting theory corresponds to the chiral clock model [25], which predicts non-zero chirality for our model. This also indicates the presence of a gapless incommensurate phase between L_1 and L_2 . For a finite chain we find strong evidence for the presence of this phase using computational simulations.

To gain a further insight into the nature of the ground states of our model we introduce the order parameter [14]

$$\Psi_p = \sum_j e^{2\pi i j/p} |\downarrow\rangle_j \langle \downarrow|, \quad (4.20)$$

that reveals the periodicity of a state. For example, its expectation value is maximal for p -periodic states, and minimal (or zero) otherwise. In particular, the wave order parameter, Ψ_3 , is a complex operator that detects the period 3 states. We wish to use Ψ_3 as an order parameter to probe the behavior of our model between the boundaries L_1 and L_2 . With this in mind we construct a continuum quantum field theory with an action that has the same symmetries as $\langle \Psi_3 \rangle$ does in the Z_3 region.

It is easy to verify that $\langle \Psi_3 \rangle$ is invariant under translations $\Psi_3 \rightarrow e^{2\pi i l/3} \Psi_3$, for integer l . A more intriguing symmetry is given when simultaneous spatial reflections and complex conjugation are performed, $x \rightarrow -x$, $\Psi_3 \rightarrow \Psi_3^*$ [26]. Finally, $\langle \Psi_3 \rangle$ is invariant under time reversal, $\tau \rightarrow -\tau$. According

to these symmetries, we can write down the corresponding effective field theory, given by,

$$\mathcal{S}_3 = \int dx d\tau \left[i\alpha \Psi_3^* \partial_x \Psi_3 + \text{c.c.} + |\partial_\tau \Psi_3|^2 + v^2 |\partial_x \Psi_3|^2 + r |\Psi_3|^2 + v \Psi_3^3 + \text{c.c.} + \dots \right]. \quad (4.21)$$

The parameters α, v and r are non-universal functions of the original λ_1 and λ_2 . It has been shown [27] that this model has a critical point at $\alpha = r = 0$ that belongs in the same universality class as the point P_3 . We may therefore identify them.

The term $\alpha \Psi_3^* \partial_x \Psi_3$ breaks chiral symmetry when Ψ_3 is complex. The resulting theory has been studied by Ostlund [25] and it has been shown that it belongs in the same universality class as the chiral clock model. Hence, it suggests the presence of a chiral phase for non-zero values of α . Furthermore this model predicts that this phase is gapless and incommensurate [26, 28]. By analogy we conjecture that our model has such a phase away from P_3 and we shall investigate it numerically.

The gapless and incommensurate characteristics of this phase indicate that $\langle \Psi_p \rangle$ can build a non-zero value by applying the appropriate perturbation. Hence, we add to the Hamiltonian a small periodic potential of the form

$$V = 10^{-4} \sum_j e^{2\pi i j/p} |\downarrow\rangle_j \langle \downarrow| \quad (4.22)$$

and we plot $\langle \Psi_p \rangle$ for several p as a function of λ_1 and λ_2 . Indeed, for $p < 3$, we find that $\langle \Psi_p \rangle \neq 0$ between L_1 and L_2 and deduce that $\alpha \neq 0$ there (see Figure 7). A naive analysis of our field theory in which we treat Ψ_p as a fluctuation of the uniform solution indicates that α may be proportional to $2\pi/p - 2\pi/3$. This suggests a region of $\alpha \neq 0$, with opposite sign corresponding to $p > 3$, in which a second chiral phase exists on the other side of P_3 . We discover numerical evidence for this in Figure 8 when $\lambda_1 < 0$ and $\lambda_2 < 1$, but its effect is of lower order than in Figure 7.

Along with the gapless incommensurate properties of this phase we would like to investigate its chiral nature. Note that, on the one hand, the chirality operator, given by $\chi_i \equiv \vec{\sigma}_i \cdot \vec{\sigma}_{i+1} \times \vec{\sigma}_{i+2}$, is an imaginary hermitian operator. On the other hand the Hamiltonian (2.1) is real. Thus, if the Hamiltonian possesses a ground state with non-zero expectation value $\langle \chi \rangle$, that ground state should be multidegenerate. If this is the case in the thermodynamic limit we would like to see if it is also approximated in the finite case. By numerical simulations we can obtain the lowest

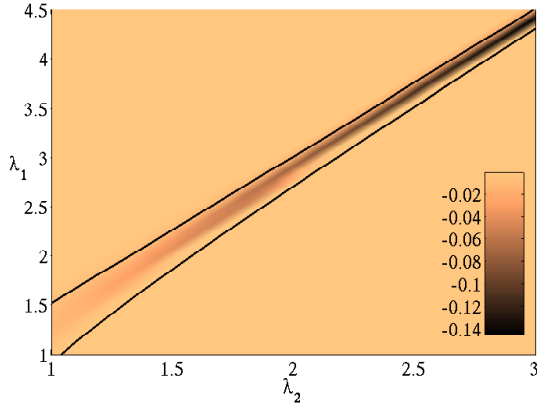


FIG. 7: Surface plot of $\langle \Psi_{18/7} \rangle$. There is a narrow band of excitation within the intermediate region predicted by perturbation theory, giving strong indication for the presence of gapless incommensurate phase.

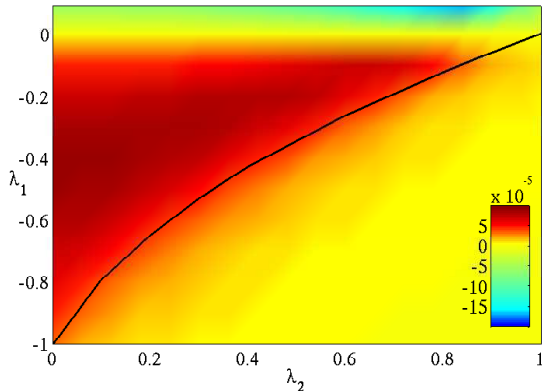


FIG. 8: This plot shows $\langle \Psi_{18/5} - \Psi_{18/7} \rangle$ over $\lambda_1 < 0, \lambda_2 < 1$. There is a clear region, bounded by the predictions of perturbation theory, where $|\psi\rangle$ responds best to excitations of spin-order $p = 18/5 > 3$, indicating, in tandem with Figure 7, a theory with $p < 3$ above P_3 and $p > 3$ below.

energy gap, ΔE , for values of the couplings λ_1 and λ_2 between the L_1 and L_2 lines. In Figure 9 we can clearly observe an exponential damping of ΔE as a function of the length of the spin chain. This allows us to assume that in the thermodynamic limit the spectrum will eventually become degenerate.

V. CONCLUSION

The present spin model approximates the behavior of the Mott insulator of two species of atoms when

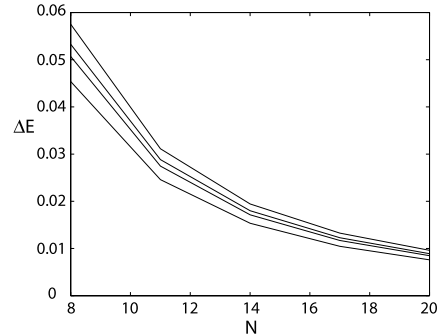


FIG. 9: The energy gap, ΔE , per site between the ground state and first excited state tends exponentially to zero as the total length of the chain increases. In the thermodynamical limit we expect to have zero energy gap. The lines correspond to different points along the $\lambda_1/\lambda_2 = 3/2$ asymptote, ordered from top to bottom the further away the points are from the origin.

a triangular ladder geometry is realized. The spin interpretation, which makes the study of the model simpler and more intuitive, is valid when there is only one atom per lattice site, i.e. at the regime of strong collisional couplings. With this condition satisfied the criticality behavior of the spin model straightforwardly represents the behavior of the Mott insulator. We can argue that non-zero chirality in the spin model corresponds to a ground state with persistent currents [29]. This suggests a counterflow of the two different atomic species that could be measured by using atomic spatial correlations [30].

To summarize, in this article, we have generalized the one-dimensional Ising model, ZZ , to include an additional triple σ^z interaction, ZZZ , in the presence of a transverse magnetic field. A rich criticality behavior has been revealed when the coupling of ZZ and ZZZ are varied. The phases of the ground state are identified according to their periodic structure. In particular, a complex order parameter related to the states with period three has revealed a chiral, gapped, incommensurate phase. In [14] a thorough study of this phase in a one-dimensional hard boson model exhibiting similar behavior was performed. An in depth study of the incommensurate phase will be the subject of a future publication.

Acknowledgments

This work was supported by the Royal Society.

-
- [1] D. Jaksch, C. Bruder, J.I. Cirac, C.W. Gardiner, and P. Zoller, Phys. Rev. Lett. **81** 3108 (1998).
- [2] A. Kastberg, W. D. Phillips, S. L. Rolston, R. J. C. Spreeuw, and P. S. Jessen, Phys. Rev. Lett. **74**, 1542 (1995); G. Raithel, W. D. Phillips, and S. L. Rolston, Phys. Rev. Lett. **81**, 3615 (1998).
- [3] M. Greiner, O. Mandel, T. Esslinger, T. W. Hänsch, and I. Bloch, Nature **415**, 39 (2002); M. Greiner, O. Mandel, T. W. Heanch, and I. Bloch, Nature **419**, 51 (2002).
- [4] O. Mandel, M. Greiner, A. Widera, T. Rom, T. W. Heanch, and I. Bloch, Nature **425**, 937 (2003).
- [5] I. H. Deutsch, G. K. Brennen and P. S. Jessen, Forsch. der Phys. (2000), quant-ph/0003022.
- [6] D. Jaksch, to appear in Contemporary Physics, quant-ph/0407048.
- [7] J. J. Garcia-Ripoll and I. J. Cirac, Phil. Trans. R. Soc. Lond. A 361, 1537-1548 (2003).
- [8] A. Kuklov, N. Prokof'ev, and B. Svistunov Phys. Rev. Lett. **92**, 050402 (2004).
- [9] B. Paredes, A. Widera, V. Murg, O. Mandel, S. Fölling, I. Cirac, G. V. Shlyapnikov, T. W. Hänsch, and I. Bloch, Nature **429**, 277 (2004).
- [10] A.B. Kuklov, and B.V. Svistunov, Phys. Rev. Lett. **90**, 100401 (2003).
- [11] D. Jaksch, and P. Zoller, New Journal Phys. **5**, 56.1 (2003).
- [12] L.M. Duan, E. Demler, and M. D. Lukin, Phys. Rev. Lett. **91**, 090402 (2003).
- [13] J. K. Pachos, and E. Rico, Phys. Rev. A **70**, 053620 (2004).
- [14] P. Fendley, K. Sengupta, and S. Sachdev, Phys. Rev. B. **69**, 75106 (2004).
- [15] C. M. Dawson, and M. A. Nielsen, Phys. Rev. A **69**, 52316 (2004).
- [16] F. Y. Wu, Rev. Mod. Phys. **54**, 235 (1982).
- [17] A. Kay, D. K. K. Lee, J. K. Pachos, M. B. Plenio, M. E. Reuter and E. Rico, Optics and Spectroscopy **99**, 355 (2005), quant-ph/0407121.
- [18] For a study of the corresponding classical model see: F. C. Alcaraz and J. C. Xavier, J. Phys. A: Math. Gen. **32** 2041 (1999); D. W. Wood and H. P. Griffiths, J. Phys. C: Solid State Phys. **5** L253 (1972).
- [19] K. A. Penson, R. Jullien, and P. Pfeuty, Phys. Rev. B **26**, 6334 (1982); K. A. Penson, J. M. Debierre, and L. Turban, Phys. Rev. B **37**, 7884 (1988).
- [20] F. Igloi, J. Phys. A **20**, 5319 (1987); Phys. Rev. B **40**, 2362 (1989); J. C. Angles d'Auriac, and F. Ingloi, Phys. Rev. E **58**, 241 (1998).
- [21] Loïc Turban, J. Phys. C **15** L65-L68 (1982); K. A. Penson, R. Jullien, and P. Pfeuty, Phys. Rev. B **26**, 6334 (1982).
- [22] N. Goldenfield, *Lectures on phase transitions and the renormalisation group*, Addison-Wesley (1992).
- [23] J. I. Latorre, E. Rico, and G. Vidal, QIC **4**, 48 (2004).
- [24] S. Sachdev, *Quantum Phase Transitions*, Cambridge University Press (2001).
- [25] S. Ostlund, Phys. Rev. B **24**, 398 (1981).
- [26] D. A. Huse and M. E. Fisher, Phys. Rev. Lett. **49**, 793 (1982).
- [27] R. J. Baxter, J. Phys. A **13**, L61 (1980); J. Stat. Phys. **26**, 427 (1981).
- [28] J. L. Cardy, Nucl. Phys. B **389**, 577 (1993).
- [29] W. Zhuo, X. Wang, and Y. Wang, cond-mat/0501693.
- [30] J. P. Grondalski, P. M. Alsing, and I. H. Deutsch, Opt. Exp. **5**, 249, (1999).